Lossless Image Coding Based on Lifting Wavelet Scheme using Cellular Neural Networks

Mayumi Iida, Nobuaki Takahashi, Tsuyoshi Otake and Mamoru Tanaka

Department of Electrical and Electronics Engineering, Sophia University
7-1 Kioi-cho, Chiyoda-ku, Tokyo 102-8554, Japan
Phone:+81-3-3238-3878, Fax:+81-3-3238-3321
Email: mayumi@mamoru.ee.sophia.ac.jp

Abstract— This paper proposes a new lossless image coding technique based on lifting wavelet scheme using cellular neural network (CNN). The main feature of the lifting is that it provides an entirely spatial domain interpolation of the transform, as opposed to the traditional frequency domain based constructions. In our method, the subsampled images are effectively interpolated by using the two layered CNN. The simulation results show a better coding performance compared with the conventional methods.

1. Introduction

Lossless signal and image compression is indispensable for many applications for which perfect accuracy is needed, such as the transmission of depth maps for the construction of three-dimensional (3D) views of a scene and most notably for the efficient storage and communication of medical images [1][2]. The lossless and associated lossy compression methods are often integrated into a progressive image transmission scheme.

In this paper, we propose lossless image coding based on non-separable 2D lifting using cellular neural network (CNN) [3][4]. The lifting scheme [5]-[8] is a new method for constructing biorthogonal wavelets. The main difference with classical constructions is that it dose not rely on the Fourier transform. It provides an entirely spatial domain interpretation of the transform, as opposed to the more traditional frequency domain based constructions. Therefore, the performance of lifting method depends on the ability of the filters to interpolate the images. In regard to the image interpolation, it is reported that the radial basis function (RBF) network is effective to interpolate the subsampled image for progressive transmission [9]. In [10], the CNN is applied to map the subsampled image into the domain concerned with the RBF network coefficients. Our goal is to obtain the better lossless coding efficiency by introducing the CNN interpolation technique to the lifting scheme.

2. Non-separable 2D lifting

In the traditional lifting scheme, the 1D filter is applied to horizontally and vertically. For example, S+P transform [10] of lossless image coding can be considered as 1D lifting. Fig.1 shows a typical lifting stage which is comprised of three steps: Split, Predict, and Update.

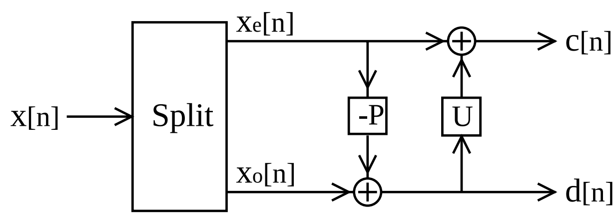

Figure 1: The lifting steps: Split, Predict, and Update.

In the case of 1D lifting, we first split the original signal $x[n]$ into its even and odd polyphase components $x_e[n]$ and $x_o[n]$, where $x_e[n] = x[2n]$ and $x_o[n] = x[2n+1]$. If the original signal correspond to the samples of an underlying smooth, slowly varying function, then the even and odd polyphase components are highly correlated. The predictor for each $x_o[n]$ is a linear combination of neighboring even coefficients,

$$P(x_e)[n] = \sum_l p_l x_e[n+l]. \tag{1}$$

Then we obtain a new representation of the $x[n]$ by replacing $x_o[n]$ with the prediction residuals,

$$d[n] = x_o[n] - P(x_e)[n]. \tag{2}$$

In the third step, we update the even polyphase coefficients $x_e[n]$ with a linear combination of the prediction residuals $d[n]$.

$$c[n] = x_e[n] + U(d)[n], \tag{3}$$

where $U(d)$ is a linear combination of neighboring d values,

$$U(d)[n] = \sum_l u_l d[n+l] \tag{4}$$

In our proposed CNN lifting, the split and the prediction steps are applied.

In order to obtain the better estimation, the 1D lifting is expanded into the non-separable 2D lifting [11]. When the 2D lifting is applied, 2D signals can be divided into two frequency components in terms of both vertical and horizontal frequency. Fig.2 shows the bandsplitting characteristic of the 2D lifting. In this case, two lifting stages are repeated alternatively (Fig.3). At the first stage, we split the signal into two components even polyphase coefficients x_{e1} and odd polyphase coefficients x_{o1} (Fig.4). Then, the predict and the update processes are applied. At the second stage, lifting three steps are applied to the low frequency components. In this case, it should be noted that the array of the low frequency components differs from the original signal. In the second split step, we divide the low frequency components into the odd line coefficients and the even line coefficients. As shown in Fig.5, we obtain a new representation $x_{e2}[m, n]$ and $x_{o2}[m, n]$. In our proposed method, the two-layered CNN is applied to perform the better prediction.

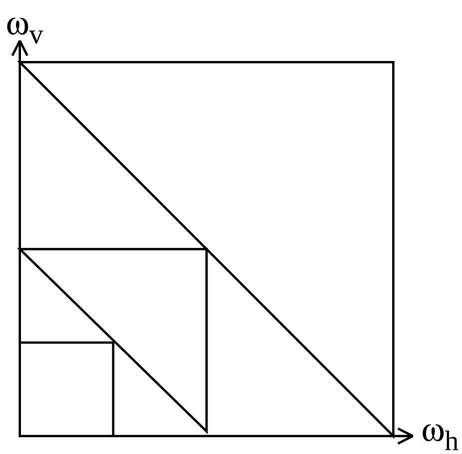

Figure 2: Bandsplitting characteristics of the non-separable 2D lifting.

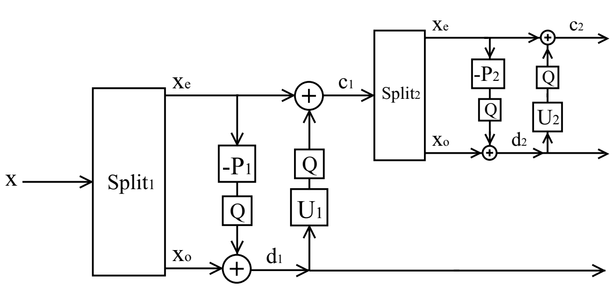

Figure 3: Structure of the 2D lifting.

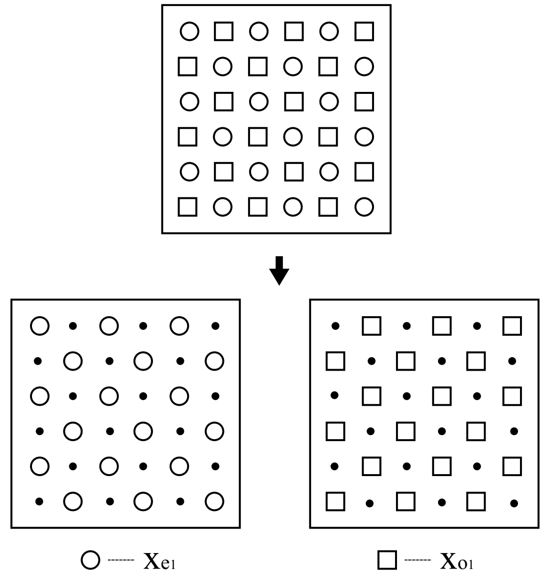

Figure 4: Split step at the first stage.

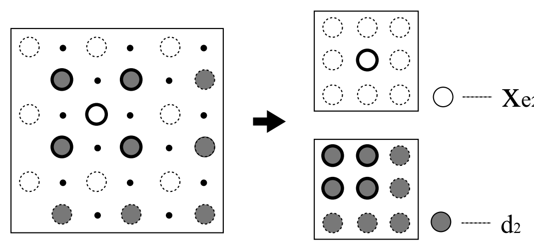

Figure 5: Split step at the second stage.

3. Lifting scheme using two-layered CNN

In the proposed method, the subsampled even polyphase images such like Fig.4 and Fig.5 are interpolated using the two-layered CNN. The even polyphase image is mapped into a domain concerned with RBF coefficients by the CNN shown in Fig.6, where the location of the pixel of the subsampled image is corresponding to the RBF center. Next, the output of the first layer CNN becomes the input of the second layer CNN which has no dynamics, and the outputs of the second layer CNN give the predicted value of the odd polyphase image.

The dynamics of the first layer CNN is represented by

$$\frac{dx_{ij}}{dt} = \sum_{C(k,l)\in N_r(i,j)} A(i,j;k,l)y_{kl}(t) + \sum_{C(k,l)\in N_r(i,j)} B(i,j;k,l)u_{kl}, \tag{5}$$

$$y_{ij}(t+1) = f\left(x_{ij}(t+1)\right), \tag{6}$$

where $N_r(i,j)$ is r-neighborhood of cell $C(i,j)$ as $N_r(i,j) = \{C(k,l)|\max\{|k-i|,|l-j|\} \le r, 1 \le k \le K_x; 1 \le l \le K_y\}$. $x_{ij}(t)$, $y_{ij}(t)$, and u_{ij} indicate the internal state, the output of the cell, and the input of the cell $C(i,j)$, respectively. $A(i,j;k,l)$ and $B(i,j;k,l)$ are the feedback and feed-forward coefficients from the neighbored cells. For mapping the even components into the RBF coefficients, the even polyphase image is set to u_{ij}. After the transition of the network, the equilibrium output y^e_{ij} is obtained as the RBF coefficient. If Gauss distribution is assumed as the RBF, the A-template $A(i,j;k,l)$ is represented by

$$A(i,j;k,l) = \begin{cases} -(1+\lambda) \\ \qquad \text{if } k=i \text{ and } l=j, \\ -\dfrac{1}{2\pi\sigma^2}\exp\left(-\dfrac{\{(k-i)^2+(l-j)^2\}d_m^2}{2\sigma^2}\right) \\ \qquad \text{otherwise.} \end{cases} \tag{7}$$

where σ is the standard derivative of the Gaussian function and λ is a regularization parameter. The B-template $B(i,j;k,l)$ is only non-zero at the center value.

$$B(i,j;k,l) = \begin{cases} 1 & \text{if } k=i \text{ and } l=j \ , \\ 0 & \text{otherwise.} \end{cases} \tag{8}$$

Using the output y^e_{ij} at the equilibrium state of the first layer CNN, the interpolated pixel $\hat{y}_{ij}$ is obtained by

$$\hat{y}_{ij} = \sum_{y_{kl} \in N'(i,j)} \hat{B}(i,j;k,l) y^e_{ij}, \tag{9}$$

where

$$\begin{aligned} \hat{B}(i,j;k,l) &= \frac{1}{2\pi\sigma^2}\exp\left(-\frac{(k-i)^2+(l-j)^2}{2\sigma^2}\right), \\ N'(i,j) &= \{C(k,l)|\max\{|k-i|,|l-j|\} \le r\}, \end{aligned} \tag{10}$$

at the odd layer stages and

$$\begin{aligned} &\hat{B}(i,j;k,l) = \frac{1}{2\pi\sigma^2} \\ &\quad \cdot \exp\left(-\frac{((k-0.5)d_m - i)^2 + ((l-0.5)d_m - j)^2}{2\sigma^2}\right), \\ &N'(i,j) = \{C(k,l)|\max\{|(k-0.5)d_m - i| \\ &\qquad ,|(l-0.5)d_m - j|\} \le (r-1)d_m + 1\}, \end{aligned} \tag{11}$$

at the even layer stages.

Fig.8 shows the block diagram of the progressive image reconstruction based on the lifting scheme using CNN interpolation. At the sprit stage, the original image u_1 is splitted into even polyphase components u_{e1} and odd polyphase components u_{o1} such like Fig.4. The prediction for each u_{on} is designed by using the two-layered CNN. Then we obtain the prediction residual e_n, that is transmitted to the decorder. In the encoder, these lifting processes using the CNN are applied to the even polyphase image iteratively. In the decoder, the same CNN lifting rules are applied, and the reconstruction image is gradually improved by adding the difference image and the interpolated components.

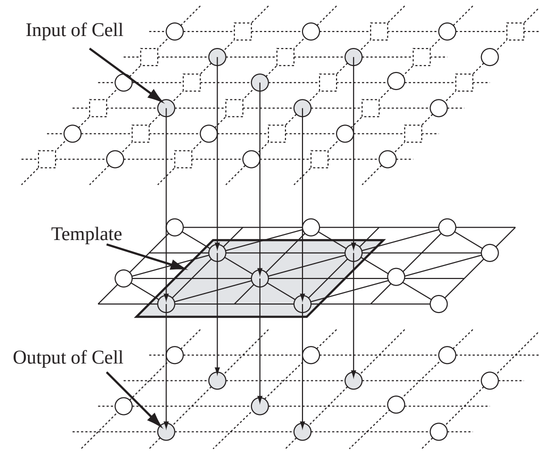

Figure 6: First layer CNN.

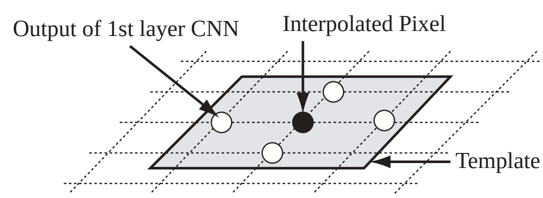

Figure 7: Second layer CNN.

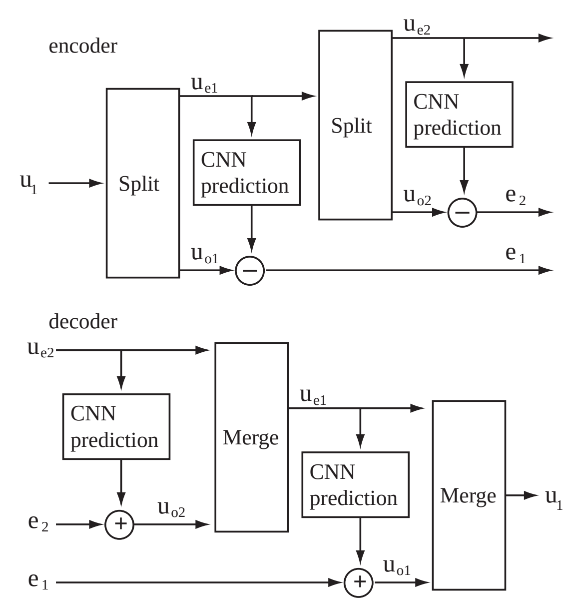

Figure 8: Proposed lossless image coding system.

Table 1: Energy of the difference images for each layer (Lena 512 $\times$ 512).

layer	1st	2nd	3rd	4th	5th	6th	7th	8th
proposed method	**20.998**	**46.017**	**92.727**	152.89	253.71	349.46	**439.40**	**636.32**
2D lifting	24.403	50.811	94.492	151.01	250.54	343.43	439.71	637.29

4. Simulation Result

Our proposed lossless image coding algorithm based on the lifting wavelet scheme using the two-layered CNN was applied to the standard gray-scale test image "Lena." The performance of the proposed method was compared with the non-separable 2D lifting method [11]. According to the simulation, the coding factor is decided as follows; the number of layers $L = 8$ and the standard deviation of Gaussian $\sigma = 0.8$. Table 1 shows the energy of the difference images for each layer. As shown in this table, our proposed method gives a better prediction performance compared with the conventional lifting method.

5. Conclusions

The lossless image coding based on the non-separable 2D lifting using the CNN was proposed. Introducing the 2D lifting with the two-layered CNN, we can show that the proposed method is superior to the conventional method using the linear filters.

References

[1] N. V. Boulgouris and M. G. Strintzis, "Orientation-sensitive interpolative pyramids for lossless and image coding," IEEE Trans. Image Processing, vol. 9, pp. 710-715, Apr. 2000.

[2] N. V. Boulgouris and M. G. Strintzis, "Optimal Progressive lossless image coding using reduced pyramids with variable decimation ratios," IEEE Trans. Image Processing, vol. 9, pp. 2117-2123, Dec. 2000.

[3] L. O. Chua and L. Yang, "Cellular neural networks: theory," IEEE Trans. Circuits Syst., vol. 35, no. 10, pp. 1257-1272, 1988.

[4] L. O. Chua and T. Roska, "The CNN paradigm," IEEE Trans. Circuits Syst., vol. 40, no. 3, pp. 147-156, 1993.

[5] I. Daubechies and W. Sweldens, "Factoring wavelet transforms into lifting steps," J. Fourier Anal. Appl., vol. 4, no. 3, pp. 245-267, 1998.

[6] R. L. Claypoole Jr., G. M. Davis and W. Sweldens, "Nonlinear wavelet transforms for image coding via lifting," IEEE Trans. Image Processing, Aug. 1999.

[7] W. Sweldens, "The lifting scheme: A custom-design construction of biorthogonal wavelets," Appl., Comput. Harmon. Anal., vol. 3, no. 2, pp. 186-200, 1996.

[8] W. Sweldens, "The lifting scheme: A construction of second generation wavelets," SIAM J. Math. Anal., vol. 29, no. 2, pp. 511-546, 1997.

[9] T. Sigitani, Y. Iiguni and H. Maeda, "Image interpolation for progressive transmission by using radial basis function networks," IEEE Trans. Neural Networks, vol. 10, no. 2, pp. 381-390, 1999.

[10] S. Itakura, Y. Tanji, T. Otake and M. Tanaka, "Progressive image reconstruction via cellular neural networks," Proc. of ISCAS2002, pp. 233-236, Phoenix, USA, May 2002.

[11] M. Iida, T. Otake, and M. Tanaka, "Lossless image coding using non-separable 2D lifting," Proc. of NOLTA2001, pp. 187-190, Miyagi, Japan, 2001.